Acta Crystallographica Section F
Structural Biology and Crystallization Communications
ISSN 1744-3091

The use of Co^{2+} for crystallization and structure determination, using a conventional monochromatic X-ray source, of flax rust avirulence protein

Gregor Gunčar,[a,b]‡§ Ching-I A. Wang,[a]‡ Jade K. Forwood,[a,b] Trazel Teh,[a] Ann-Maree Catanzariti,[c] Jeffrey G. Ellis,[c] Peter N. Dodds[c] and Boštjan Kobe[a,b,d]*

[a]School of Molecular and Microbial Sciences, University of Queensland, Brisbane, Qld 4072, Australia, [b]Institute of Molecular Bioscience, University of Queensland, Brisbane, Qld 4072, Australia, [c]Division of Plant Industry, Commonwealth Science and Industrial Research Organisation, Canberra, ACT 0200, Australia, and [d]Special Research Centre (SRC) for Functional and Applied Genomics, University of Queensland, Brisbane, Qld 4072, Australia

‡ These authors contributed equally to this work.
§ On leave from the Department of Biochemistry and Molecular Biology, Josef Stefan Institute, Ljubljana, Slovenia.

Correspondence e-mail: b.kobe@uq.edu.au

Received 14 November 2006
Accepted 29 January 2007

PDB Reference: AvrL567-A, 2opc, r2opcsf.

Metal-binding sites are ubiquitous in proteins and can be readily utilized for phasing. It is shown that a protein crystal structure can be solved using single-wavelength anomalous diffraction based on the anomalous signal of a cobalt ion measured on a conventional monochromatic X-ray source. The unique absorption edge of cobalt (1.61 Å) is compatible with the Cu $K\alpha$ wavelength (1.54 Å) commonly available in macromolecular crystallography laboratories. This approach was applied to the determination of the structure of *Melampsora lini* avirulence protein AvrL567-A, a protein with a novel fold from the fungal pathogen flax rust that induces plant disease resistance in flax plants. This approach using cobalt ions may be applicable to all cobalt-binding proteins and may be advantageous when synchrotron radiation is not readily available.

1. Introduction

Multiple-wavelength anomalous diffraction (MAD) and single-wavelength anomalous diffraction (SAD) are methods that are commonly used to solve the phase problem as part of protein structure determination by X-ray crystallography (Hendrickson & Teeter, 1981; Wang, 1985; Hendrickson, 1991; Guss *et al.*, 1988; Dauter, 2002; Dauter *et al.*, 2002; Dodson, 2003). MAD and SAD methods are often used in combination with selenomethionine-labelled proteins in order to avoid the uncertain and time-consuming screening for heavy-atom binding. However, MAD/SAD methods based on the anomalous signal from Se and many other commonly used heavy atoms require the use of a synchrotron-radiation source so that appropriate wavelengths near the absorption edges of these atoms can be selected. SAD has certain advantages over MAD as it reduces the use of beam time and thus minimizes crystal decay. Many protein structures have been successfully determined by SAD phasing using a variety of heavy atoms and either in-house X-rays or synchrotron radiation (Hendrickson & Teeter, 1981; Wang, 1985; Hendrickson, 1991; Guss *et al.*, 1988; Dauter, 2002; Dauter *et al.*, 2002; Dodson, 2003).

Here, we show that the anomalous signal resulting from cobalt ions bound in protein crystals can be used to solve the phase problem with SAD techniques using radiation from a conventional copper-anode X-ray source. This approach overcomes the disadvantages of using S atoms for SAD phasing, including the requirement for a chromium anode, and reduces the need for extremely accurate measurements of the anomalous signal. The use of cobalt also avoids the toxicity and cost of many conventional heavy-atom compounds. In addition, it has been demonstrated that cobalt can be substituted in metalloproteins for other metal ions that have similar binding geometry and coordination (Glusker, 1991; Harding, 2004; Maret & Vallee, 1993), such as zinc (Vallee *et al.*, 1958; Vallee, 1973; Maret & Vallee, 1993; Hartwig, 2001; Ghering *et al.*, 2004), iron (Sugiura *et al.*, 1975) and copper (Calabrese *et al.*, 1972). The proteins with the substituted metal often retain their native biological activity (Maret & Vallee, 1993). As metal-binding sites are ubiquitous in proteins, the method should be broadly applicable: one-third to one-half of all proteins have been estimated to bind metals (Tainer *et al.*, 1992) and zinc enzymes outnumber any other group of metalloenzymes (Maret & Vallee,

1993). While the anomalous signal arising from cobalt ions has been used previously to solve macromolecular structures using synchrotron (Borths *et al.*, 2002; Sussman *et al.*, 2000; Sauvage *et al.*, 2005) or Cu $K\alpha$ (Batey *et al.*, 2004; Vedadi *et al.*, 2007; PDB code 2f7n) radiation, we suggest that this approach could be more generally applicable to a wide range of proteins.

We demonstrate the utility of the method by determining a novel crystal structure, that of the avirulence protein AvrL567-A from the fungal pathogen *Melampsora lini*. Avirulence proteins trigger the resistance response in plants by interacting with plant disease-resistance (R) proteins as part of the gene-for-gene resistance process (Flor, 1971). AvrL567-A is specific for flax (*Linum usitatissimum*) plants carrying the L5, L6 or L7 resistance genes (Dodds *et al.*, 2004, 2006). The structure of AvrL567-A was determined at 2 Å resolution (and refined at 1.4 Å resolution) and reveals a novel β-barrel-like fold.

2. Materials and methods

2.1. Expression and purification

The AvrL567-A protein (residues 24–150; the signal peptide was not included) was produced in *Escherichia coli* as a fusion protein with N-terminal hexahistidine (His tag) and ubiquitin tags (Catanzariti *et al.*, 2004; Dodds *et al.*, 2006). For bacterial expression, the expression plasmid was transformed into *E. coli* strain BL21(DE3) by heat shock and grown aerobically at 310 K in LB broth to an OD_{600} of 0.8–1.0. IPTG (isopropyl thiogalactoside; 1 m*M*) was added to induce expression at 288 K for a further 18–20 h (final OD_{600} = 2.5–3.0). The cells were harvested by centrifugation at 6700*g* for 10 min at 277 K and resuspended in 1/10 of the culture volume in buffer *A* [20 m*M* HEPES–NaOH pH 7, 300 m*M* NaCl, 10 m*M* imidazole, 1 m*M* PMSF (phenylmethylsulfonyl fluoride), 1 mg ml^{-1} aprotinin, 1 mg ml^{-1} leupeptin, 1 mg ml^{-1} pepstatin]. Cell suspensions were lysed by repeated freeze–thaw cycles in liquid nitrogen with the addition of lysozyme (0.5 mg ml^{-1}) and DNase (50 units per 50 ml of lysate; Roche). Cell debris was removed by centrifugation at 15 000*g* for 30 min. The soluble fractions were collected and incubated with Talon resin (2 ml pre-washed in buffer *A* resin per litre of culture; BD Biosciences) for immobilized metal-affinity chromatography (IMAC). After 1 h incubation on a rotating wheel at 277 K, the resin was washed with buffer *A* and buffer *B* (buffer *A* containing 20 m*M* imidazole) and finally resuspended in 13 ml of buffer *A* containing deubiquitinating (DUB) enzyme (1:50 enzyme:substrate ratio) and 5 m*M* β-mercaptoethanol for 18–20 h at 277 K. The cleaved AvrL567-A containing no fusion tags was then eluted in the supernatant and further purified by size-exclusion chromatography (in a buffer containing 20 m*M* HEPES–NaOH pH 7, 300 m*M* NaCl) using a Hi-Load Superdex 200 26/60 gel-filtration column (GE Healthcare). Purified AvrL567-A protein was concentrated to ∼30 mg ml^{-1} using Amicon Ultra centrifugal filter devices with low-binding Ultracel membranes (Millipore), frozen as aliquots in liquid nitrogen and stored at 193 K. The protein concentrations were determined by measuring the absorption at 280 nm based on the calculated extinction coefficient (21 030 M^{-1} cm^{-1}). The final yield was approximately 10 mg protein per litre of culture. The protein was more than 95% pure as determined by SDS–PAGE. DUB was expressed as described for AvrL567-A, except that the overnight culture was grown at 310 K, purified on Talon resin washed with both buffer *A* and buffer *B* containing 5 m*M* β-mercaptoethanol and eluted with buffer *C* (buffer *A* containing 150 m*M* imidazole and 5 m*M* β-mercaptoethanol; Catanzariti *et al.*, 2004), concentrated to 5 mg ml^{-1} and stored as AvrL567-A.

Table 1
Diffraction data-collection and refinement statistics.

Values in parentheses are for the highest resolution shell.

	Data set used for phasing	Data set used for refinement
Data-collection statistics		
Reservoir solution	0.1 *M* imidazole pH 7, 4% PEG 8000, 12.5 m*M* $CoCl_2$	0.1 *M* imidazole pH 8, 4% PEG 8000
Space group	$P2_12_12_1$	$P2_12_12_1$
Unit-cell parameters (Å)		
a	39.7	39.8
b	52.3	52.4
c	70.7	70.8
Resolution range (Å)	50.0–2.01 (2.08–2.01)	50.0–1.43 (1.468–1.432)
No. of observations	266452	337806
No. of unique reflections	10313	28149
Average redundancy	14.3 (13.9)	12.1 (10.4)
Completeness (%)	97.9 (95.4)	99.1 (93.3)
Total linear $R_{\rm merge}$†	0.044 (0.150)	0.056 (0.238)
Average $I/\sigma(I)$	28.7 (17.9)	33.7 (13.95)
Refinement		
Resolution (Å)		26.5–1.43 (1.468–1.432)
No. of reflections		26436
$R_{\rm cryst}$‡		0.198 (0.412)
$R_{\rm free}$‡		0.226 (0.433)
No. of non-H atoms		
Protein		929
Solvent		196
Mean *B* factor (Å^2)		32.1
Coordinate error§ (Å)		0.198
R.m.s. deviations from ideal values		
Bond lengths (Å)		0.015
Bond angles (°)		1.617
Ramachandran plot¶, residues in		
Most favoured regions (%)		90.6
Disallowed regions (%)		0

† $R_{\rm merge} = \sum_{hkl}[\sum_i(|I_{hkl,i} - \langle I_{hkl}\rangle|)]/\sum_{hkl,i}\langle I(hkl)\rangle$, where $I_{hkl,i}$ is the intensity of an individual measurement of the reflection with Miller indices *hkl* and $\langle I_{hkl}\rangle$ is the mean intensity of that reflection, calculated for $I > -3\sigma(I)$. ‡ $R_{\rm cryst} = \sum_{hkl}(||F_{hkl}^{\rm obs}| - |F_{hkl}^{\rm calc}||)/\sum|F_{hkl}^{\rm obs}|$, where $|F_{hkl}^{\rm obs}|$ and $|F_{hkl}^{\rm calc}|$ are the observed and calculated structure-factor amplitudes. $R_{\rm free}$ is equivalent to $R_{\rm cryst}$ but calculated with reflections (5%) omitted from the refinement process. § Calculated based on a Luzzati plot using the program *SFCHECK* (Vaguine *et al.*, 1999). ¶ Calculated using the program *PROCHECK* (Laskowski *et al.*, 1993).

2.2. Protein characterization

For mass spectrometry, samples were desalted using chloroform precipitation and resuspended in 50%(*v*/*v*) acetonitrile/0.1%(*v*/*v*) acetic acid. The samples were then applied to a sinapinic acid matrix, where a 1 µl aliquot of protein sample was mixed with 1–4 µl matrix. MALDI–TOF (matrix-assisted laser desorption ionization time-of-flight mass spectrometry) was then carried out using a Voyager-DE Biospectrometry Workstation.

For N-terminal sequencing, proteins were transferred onto PVDF membrane (GE Healthcare) and stained with Ponceau S. The band at the correct molecular weight was excised and analysed with a PE Applied Biosystems Procise 492 cLC Protein Sequencer. Both MALDI–TOF and N-terminal sequencing confirmed the identity and accurate molecular weight of the protein.

The oligomeric status of the proteins was characterized by size-exclusion chromatography using the procedures described in §2.1; 100 µg of protein was incubated with 50 m*M* $CoCl_2$ for 1 h before loading onto the column. 1 m*M* EDTA was added to the oligomeric protein to confirm that cobalt was responsible for the observed effect.

2.3. Crystallization

A suitable protein concentration for crystallization screens was estimated to be 17 mg ml^{-1}, based on the behaviour with solutions No. 4 and 6 from Crystal Screen (Hampton Research). Crystallization conditions were screened using Crystal Screen, Crystal Screen 2 and Index Screen (Hampton Research), PACT Premier (Molecular Dimensions Limited), 'core screen' (Page *et al.*, 2003), Wizard I and II and Precipitant Synergy Primary 64 (Emerald BioSystems) using the hanging-drop vapour-diffusion method and a Mosquito crystallization robot (TTP LabTech, UK). Droplets containing 0.2 µl protein sample and 0.2 µl reservoir solution were equilibrated against 100 µl reservoir solution (at 277 and 290 K). Initial crystals were obtained in 10%(*v*/*v*) 2-propanol, 0.1 *M* imidazole pH 8.0 and in 10%(*w*/*v*) PEG 8000, 0.1 *M* imidazole pH 8.0 (Wizard Screen II conditions). The Fluidigm screen was also used in combination with Topaz chips for crystallization screening (Fluidigm, CA, USA), but did not yield any crystals. Optimization of crystals was performed by varying the pH, temperature and the size of the drop and the concentration of the precipitants, salts and proteins in 24-well plate format. Crystals of AvrL567-A were grown under several conditions, with the best crystals of approximately 0.3 × 0.4 × 0.3 mm obtained in 10%(*w*/*v*) PEG 8000 and 0.1 *M* imidazole/NaOH pH 8.0.

For cocrystallization with cobalt, the optimal conditions were obtained by varying the pH of the buffer and the concentrations of protein, precipitant and $CoCl_2$. The best crystals were grown in 4–10% PEG 8000, 0.1 *M* imidazole pH 7.5–8.5 and 12.5–17.5 m*M* $CoCl_2$ using a protein concentration of 25–35 mg ml^{-1}. Crystals appeared a few minutes after initial set up and the optimal size for X-ray diffraction data collection was determined to be 0.1 × 0.2 × 0.1 mm.

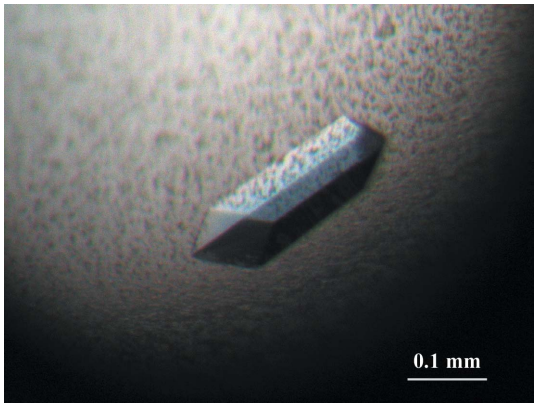

Figure 1
Representative crystal of Co-AvrL567-A grown in 10% PEG 8000, 0.1 *M* imidazole pH 8.5 and 17.5 m*M* $CoCl_2$. The blue colour suggested tetrahedral Co^{2+} coordination.

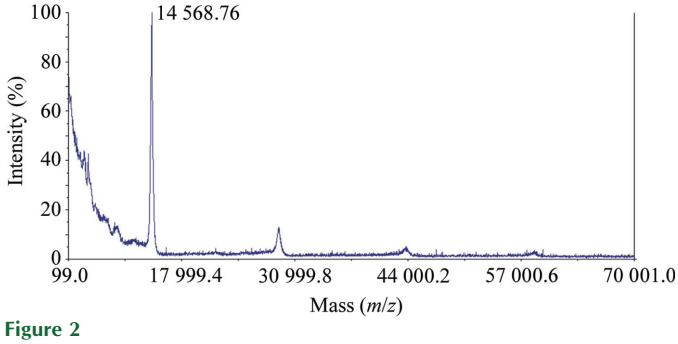

Figure 2
The incorporation of cobalt can be detected by MALDI–TOF mass spectrometry. The result shows the cobalt:protein stoichiometry to be 1:1. The error of the measurement is less than 1 Da (the cobalt-bound AvrL567-A has a molecular weight of 14 568.41 Da).

2.4. Diffraction data collection

The cobalt-containing AvrL567-A (hereafter referred to as Co-AvrL567-A) crystals were transferred into a cryoprotectant solution consisting of the crystallization mother liquor containing an additional 30%(*v*/*v*) MPD (2-methyl-2,4-pentanediol) and were flash-cooled in liquid nitrogen. The X-ray diffraction data sets were collected in a cryostream (100 K) using an R-AXIS IV^{++} image-plate detector and Cu $K\alpha$ radiation from a Rigaku FR-E rotating-anode generator (Rigaku/MSC, Texas, USA). 360° of data (1° oscillations; 10 min per exposure) were collected at a crystal-to-detector distance of 150 mm. The raw data sets were autoindexed, integrated and scaled using the *HKL*-2000 package (Otwinowski & Minor, 1997); the mosaicity was estimated at 0.384°. The crystals have the symmetry of the orthorhombic space group $P2_12_12_1$, with one molecule per asymmetric unit [corresponding to a solvent content of 51.2% and a Matthews coefficient (Matthews, 1968) of 2.5 Å^3 Da^{-1}; Table 1]. A higher resolution data set collected subsequently (360° of data, 1° oscillations, 6 min per exposure, crystal-to-detector distance of 70 mm) and processed as above (mosaicity 0.338°) was used for the refinement of the structure at 1.4 Å resolution.

2.5. Structure determination

Initially, the presence of Co^{2+} was detected using the program *HySS* (Adams *et al.*, 2002; Grosse-Kunstleve & Adams, 2003). One solution was found with *SOLVE* (Terwilliger & Berendzen, 1999), with 100% relative occupancy of the Co^{2+} atom, a figure of merit of 0.43 and an overall *SOLVE Z* score of 9.85. Three other small anomalous peaks that correspond to S atoms were found, but were not used in phasing; only the position of the Co atom was used to determine the phases with *SOLVE*. Model building was performed using *RESOLVE* (Terwilliger, 2000, 2002), *ARP*/*wARP* (Morris *et al.*, 2003) and *MAIN* (Turk, 1992), and *REFMAC* was used for refinement (Murshudov *et al.*, 1997). Water molecules were built using *ARP*/*wARP* (Morris *et al.*, 2003).

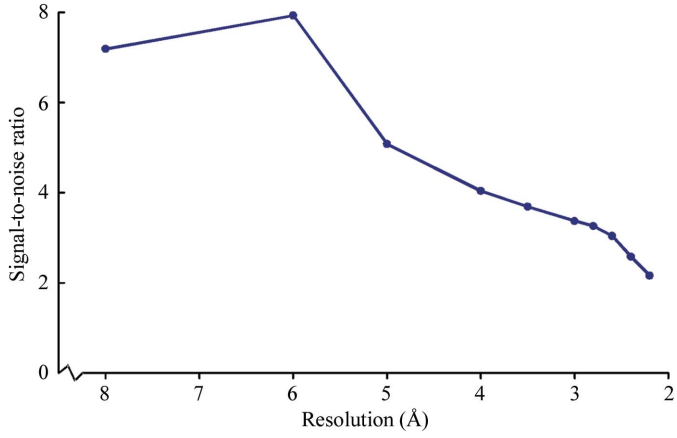

Figure 3
Resolution-dependence of the anomalous signal-to-noise ratio as calculated using the program *SHELXC* (Schneider & Sheldrick, 2002).

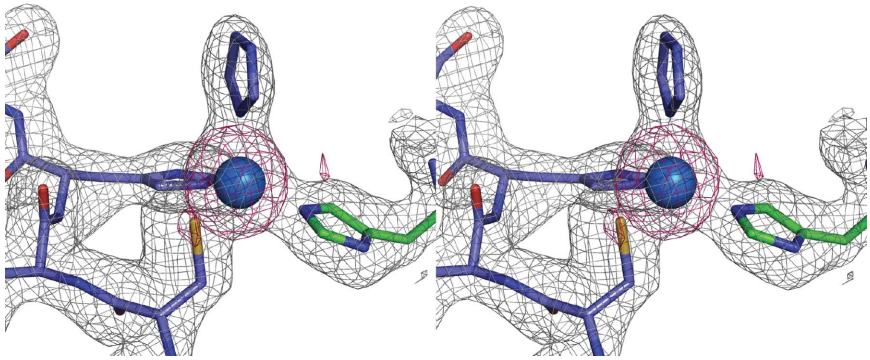

Figure 4
The tetrahedral cobalt coordination-facilitated crystal contacts. The figure shows a stereoview of the SAD electron density (following density modification with *DM* and *RESOLVE*) at 2.0 Å resolution contoured at 1.0σ (black) and the anomalous map contoured at 5.0σ (magenta); superimposed is the refined model of AvrL567-A shown in stick representation. Cobalt is shown as a green sphere and C atoms from the symmetry-related molecule are shown in green, otherwise they are shown in light blue; N, O and S atoms are shown in dark blue, red and yellow, respectively. The imidazole molecule at the top comes from the crystallization solution.

3. Results

The AvrL567-A protein was produced as a His-tagged ubiquitin-fusion protein. The N-terminal His-tagged ubiquitin was subsequently removed during the purification stage through cleavage with DUB. The initial crystals of the protein (the predicted mature protein lacking the signal peptide and containing no fusion tags) were obtained at both 277 and 290 K within 2–3 d of crystallization setup. The crystals were difficult to reproduce subsequently using new preparations of the protein. We reasoned that variability in the cobalt leakage from the Talon resin used in affinity purification could have played a role in crystallization. Indeed, addition of cobalt to the crystallization solution restored crystal growth (Fig. 1). At high cobalt concentrations, the crystals were coloured blue, suggesting specific binding of Co^{2+} with tetrahedral coordination (Cotton & Wilkinson, 1980). The incorporation of cobalt was also detected using MALDI–TOF mass spectrometry, indicating a 1:1 cobalt:AvrL567-A stoichiometry (Fig. 2). Cobalt induced the monomeric protein to dimerize, as suggested by size-exclusion chromatography.

The sequence of AvrL567-A showed no significant similarity to any protein of known structure (using *BLAST*; Altschul *et al.*, 1997). The presence of cobalt in the crystals suggested the option of using this heavy atom for phase determination. The absorption edge of cobalt (1.61 Å) is very close to the wavelength of Cu $K\alpha$ (1.54 Å; at this wavelength, f'' is expected to be 3.6 e). Therefore, we collected diffraction data for Co-AvrL567-A using our in-house X-ray source. A significant anomalous signal was observed (Fig. 3) and the structure was solved using SAD at 2 Å resolution.

The electron-density map of Co-AvrL567-A showed that Co^{2+} interacted in a tetrahedral coordination with residues His85 (2.0 Å) and Cys83 (2.3 Å) of one AvrL567-A molecule, His105 (2.0 Å) from the neighbouring AvrL567-A molecule in the crystal and one imidazole molecule (2.0 Å; Fig. 4). The structure of AvrL567-A shows a novel β-barrel-like fold.

4. Discussion

Phase determination using cobalt ions has several advantages over other phasing strategies: (i) its absorption edge at 1.61 Å allows the anomalous signal to be collected using Cu $K\alpha$ radiation (1.54 Å), (ii) most laboratories do not have access to an X-ray source with a chromium anode, (iii) only one data set measured at Cu $K\alpha$ wavelength is required, (iv) cobalt compounds are cheap and less toxic than most other heavy-atom compounds, (v) the type of coordination and the incorporation of cobalt can be distinguished by the colour of crystals (Cotton & Wilkinson, 1980) and (vi) the incorporation can easily be detected by MALDI–TOF mass spectrometry (see Fig. 2). From the data we collected using our in-house X-ray source, a significant anomalous signal generated by the cobalt ion was observed (Fig. 3) and one fully occupied cobalt-binding site was identified. The electron-density map clearly shows tetrahedral coordination by two histidine residues, a cysteine residue and an imidazole molecule (Fig. 4), consistent with the observed blue colour of the crystals. The structure shows how cobalt facilitated crystallization by connecting two molecules in the crystal.

Cobalt is a ubiquitous protein-binding metal (Maret & Vallee, 1993). One third to one half of all proteins are expected to bind metal ions (Tainer *et al.*, 1992) and cobalt can be substituted for many other naturally occurring metal ions such as zinc, iron and copper (Maret & Vallee, 1993). It could be useful to take advantage of the unique absorption edge of cobalt (1.61 Å), which is compatible with the Cu $K\alpha$ wavelength (1.54 Å) commonly available in macromolecular crystallography laboratories. Cobalt also binds to His tags, which are frequently used as affinity tags for proteins undergoing structural studies. While the tags are rarely ordered in the crystals (the following structures in the PDB have His tags included in the model: 2f0a, 1hz5, 2a0k, 1ig3, 1lw6, 1tm1, 1xtf), this may be a consequence of the flexible linker between the tag and the protein of interest. The use of cobalt as an anomalous scatterer, including the combination of cobalt and a His tag (rigidified by using a short linker), may be a generally applicable method of phase determination in protein crystals. Although this remains to be tested, we hope that our discussion will stimulate researchers to consider such methods on their favourite proteins.

5. Conclusion

Our work demonstrates that SAD phasing based on Co atoms is a convenient structure-determination strategy for macromolecular crystallography. We applied this strategy to determining the structure of *M. lini* AvrL567-A, a protein with a novel fold, by cocrystallization with cobalt and using solely in-house Cu $K\alpha$ X-ray radiation.

We acknowledge Chris Wood for the help with N-terminal sequencing and the members of the laboratory for help with data collection, crystallization and cryo-techniques. This work was supported by the Australian Research Council (ARC); BK is an ARC

Federation Fellow and a National Health and Medical Research Council of Australia (NHMRC) Honorary Research Fellow and JKF was an NHMRC C. J. Martin Fellow.

References

Adams, P. D., Grosse-Kunstleve, R. W., Hung, L. W., Ioerger, T. R., McCoy, A. J., Moriarty, N. W., Read, R. J., Sacchettini, J. C., Sauter, N. K. & Terwilliger, T. C. (2002). *Acta Cryst.* D**58**, 1948–1954.

Altschul, S. F., Madden, T. L., Schaffer, A. A., Zhang, J., Zhang, Z., Miller, W. & Lipman, D. J. (1997). *Nucleic Acids Res.* **25**, 3389–3402.

Batey, R. T., Gilbert, S. D. & Montange, R. K. (2004). *Nature (London)*, **432**, 411–415.

Borths, E. L., Locher, K. P., Lee, A. T. & Rees, D. C. (2002). *Proc. Natl Acad. Sci. USA*, **99**, 16642–16647.

Calabrese, L., Rotilio, G. & Mondovi, B. (1972). *Biochim. Biophys. Acta*, **263**, 827–829.

Catanzariti, A. M., Soboleva, T. A., Jans, D. A., Board, P. G. & Baker, R. T. (2004). *Protein Sci.* **13**, 1331–1339.

Cotton, F. A. & Wilkinson, G. (1980). *Advanced Inorganic Chemistry*, 4th ed. New York: John Wiley & Sons.

Dauter, Z. (2002). *Curr. Opin. Struct. Biol.* **12**, 674–678.

Dauter, Z., Dauter, M. & Dodson, E. (2002). *Acta Cryst.* D**58**, 494–506.

Dodds, P. N., Lawrence, G. J., Catanzariti, A. M., Ayliffe, M. A. & Ellis, J. G. (2004). *Plant Cell*, **16**, 755–768.

Dodds, P. N., Lawrence, G. J., Catanzariti, A. M., Teh, T., Wang, C. I., Ayliffe, M. A., Kobe, B. & Ellis, J. G. (2006). *Proc. Natl Acad. Sci. USA*, **103**, 8888–8893.

Dodson, E. (2003). *Acta Cryst.* D**59**, 1958–1965.

Flor, H. (1971). *Annu. Rev. Phytopathol.* **9**, 275–296.

Ghering, A. B., Shokes, J. E., Scott, R. A., Omichinski, J. G. & Godwin, H. A. (2004). *Biochemistry*, **43**, 8346–8355.

Glusker, J. P. (1991). *Adv. Protein Chem.* **42**, 1–76.

Grosse-Kunstleve, R. W. & Adams, P. D. (2003). *Acta Cryst.* D**59**, 1966–1973.

Guss, J. M., Merritt, E. A., Phizackerley, R. P., Hedman, B., Murata, M., Hodgson, K. O. & Freeman, H. C. (1988). *Science*, **241**, 806–811.

Harding, M. M. (2004). *Acta Cryst.* D**60**, 849–859.

Hartwig, A. (2001). *Antioxid. Redox Signal.* **3**, 625–634.

Hendrickson, W. A. (1991). *Science*, **254**, 51–58.

Hendrickson, W. A. & Teeter, M. A. (1981). *Nature (London)*, **290**, 107–113.

Laskowski, R. A., MacArthur, M. W., Moss, D. S. & Thornton, J. M. (1993). *J. Appl. Cryst.* **26**, 283–291.

Maret, W. & Vallee, B. L. (1993). *Methods Enzymol.* **226**, 52–71.

Matthews, B. W. (1968). *J. Mol. Biol.* **33**, 491–497.

Morris, R. J., Perrakis, A. & Lamzin, V. S. (2003). *Methods Enzymol.* **374**, 229–244.

Murshudov, G. N., Vagin, A. A. & Dodson, E. J. (1997). *Acta Cryst.* D**53**, 240–255.

Otwinowski, Z. & Minor, W. (1997). *Methods Enzymol.* **276**, 307–326.

Page, R., Grzechnik, S. K., Canaves, J. M., Spraggon, G., Kreusch, A., Kuhn, P., Stevens, R. C. & Lesley, S. A. (2003). *Acta Cryst.* D**59**, 1028–1037.

Sauvage, E., Herman, R., Petrella, S., Duez, C., Bouillenne, F., Frere, J. M. & Charlier, P. (2005). *J. Biol. Chem.* **280**, 31249–31256.

Schneider, T. R. & Sheldrick, G. M. (2002). *Acta Cryst.* D**58**, 1772–1779.

Sugiura, Y., Ishizu, K. & Kimura, T. (1975). *Biochemistry*, **14**, 97–101.

Sussman, D., Nix, J. C. & Wilson, C. (2000). *Nature Struct. Biol.* **7**, 53–57.

Tainer, J. A., Roberts, V. A. & Getzoff, E. D. (1992). *Curr. Opin. Biotechnol.* **3**, 378–387.

Terwilliger, T. C. (2000). *Acta Cryst.* D**56**, 965–972.

Terwilliger, T. C. (2002). *Acta Cryst.* D**58**, 1937–1940.

Terwilliger, T. C. & Berendzen, J. (1999). *Acta Cryst.* D**55**, 849–861.

Turk, D. (1992). PhD thesis. Technische Universitat München, Germany.

Vaguine, A. A., Richelle, J. & Wodak, S. J. (1999). *Acta Cryst.* D**55**, 191–205.

Vallee, B. L. (1973). *Adv. Exp. Med. Biol.* **40**, 1–12.

Vallee, B. L., Rupley, J. A., Coombs, T. L. & Neurath, H. (1958). *J. Am. Chem. Soc.* **80**, 4750–4751.

Vedadi, M. *et al.* (2007). *Mol. Biochem. Parasitol.* **151**, 100–110.

Wang, B.-C. (1985). *Methods Enzymol.* **115**, 90–112.